DEVELOPMENT OF CONTINUOUS SOLVENT EXTRACTION PROCESSES FOR COAL DERIVED CARBON PRODUCTS

DE-FC26-03NT41873

Quarterly Report

PERIOD OF PERFORMANCE:
October 1, 2005 - December 31, 2005

Submission date:
March 7, 2006

Principal Investigator:
Elliot B. Kennel

Co-Investigators:
Quentin C. Berg, Stephen P. Carpenter, Dady Dadyburjor, Jason C. Hissam, Manoj Katakdaunde, Liviu Magean, Abha Saddawi, Alfred H. Stiller, John W. Zondlo

West Virginia University
Department of Chemical Engineering
College of Engineering and Mineral Resources
PO Box 6102
Morgantown WV 26506

Subcontractors:
GrafTech International
12900 Snow Road
Parma, OH 44130

Koppers Inc.
1005 William Pitt Way
Pittsburgh, PA 15238

DISCLAIMER:

ABSTRACT

The purpose of this DOE-funded effort is to develop continuous processes for solvent extraction of coal for the production of carbon products. The largest applications are those which support metals smelting, such as anodes for aluminum smelting and electrodes for arc furnaces. Other carbon products include materials used in creating fuels for the Direct Carbon Fuel Cell, metals smelting, especially in the aluminum and steel industries, as well as porous carbon structural material referred to as “carbon foam” and carbon fibers.

During this reporting period, efforts have focused on the development of carbon electrodes for Direct Carbon Fuel Cells (DCFC), and on carbon foam composites used in ballistic armor, as well as the hydrotreatment of solvents used in the basic solvent extraction process. A major goal is the production of 1500 pounds of binder pitch, corresponding to about 3000 pounds of hydrotreated solvent.

Table of Contents

List of Figures

List of Tables

1.0 Executive Summary

The purpose of this DOE-funded effort is to develop continuous processes for solvent extraction of coal for the production of carbon products. These carbon products include materials used in creating fuels for the Direct Carbon Fuel Cell, metals smelting, especially in the aluminum and steel industries, as well as porous carbon structural material referred to as “carbon foam” and carbon fibers.

During this reporting period, efforts have focused on the development of carbon composites. Composite electrodes were fabricated for use as a carbon fuel cell electrode. Carbon foam samples were tested for armor applications.

2.0 Technical

2.1 Composite Electrode Rods

As a specific type of coal-derived carbon composite, electrode rods were fabricated using extracted coal as well as binder pitch. Such rods may be useful for Direct Carbon Fuel Cells (DCFC) or other applications requiring conductive carbon electrodes.[1]

A basic protocol was developed for fabricating electrodes in the shape of a rod. Briefly, carbonaceous ingredients (such as coke) were blended into a homogeneous mixture. They were then packed into a cylindrical shaped clamshell mold. The mold is heated to 210 ºC/min and kept there for 1 hour, so that the pitch softens, a piston is vertically inserted into the mold and the piston and mold are pressed in a Carver press as shown in Figure 1.

Figure 1. Clamshell Mold in a Carver Hydraulic Press [1]

The fuel mixture is pressed to 5000 lbs and allowed to cool under pressure. “After cooling, the pressure is released, the bolts are loosened and removed, and the two

sides of the mold are separated" and the fuel rod is extracted. Figure 2 shows an open mold with a carbon fuel rod in it.

Figure 2. Carbon Electrode Rod Within An Opened Mold [1]

Figure 3 depicts a green (pre-coked) carbon rod after it has been extracted from the mold. Following extraction the Carbon Fuel Rods are calcined at 1000 ºC.

Figure 3. Green Carbon Fuel Rod

Initially, rods were made with Koppers binder pitch and petcoke supplied by Science Applications Research Associates (SARA) only. This petcoke is believe to be fuel grade, rather than anode grade. SARA also supplied an extracted carbon referred to as Cenfuel, from Carbonxt, Charleston, WV. Rods of the following compositions were manufactured:

0% Cenfuel, 100% Petroleum Coke
25% Cenfuel, 75% Petroleum Coke
50% Cenfuel, 50% Petroleum Coke
80% Cenfuel, 20% Petroleum Coke
100% Cenfuel, 0% Petroleum Coke

All rods were manufactured with 15% Kopppers binder pitch (standard anode grade) by weight.

Just as with Cenfuel, rods with varying amounts of Solvent Extracted Carbon Ore (SECO) and petroleum coke were created to determine the lowest amount of petcoke that can be tolerated while keeping electrical conductivity high.

The rods that were fabricated are as follows:

0% SECO, 100% Petroleum Coke
25% SECO, 75% Petroleum Coke
50% SECO, 50% Petroleum Coke
75% SECO, 25% Petroleum Coke
100% SECO, 0% Petroleum Coke

All rods were manufactured with 15% Koppers binder pitch by weight.

2.1.1 Composite Electrical Resistivity Measurements

The solid carbon composite rods must be electrically conductive because they act as the anode in the DCFC employed in this research. To measure the resistivity of the rods, ASTM C 611 "Standard Test Method for Electrical Resistivity of Manufactured Carbon and Graphite Articles at Room Temperature" was followed. To that end, a four point system was assembled consisting of a power supply, current meter, variable resistor, volt meter, and a carbon rod holder that has two copper plates on both ends for electrical contact with the rod. The assembled system is shown in Figure 4.

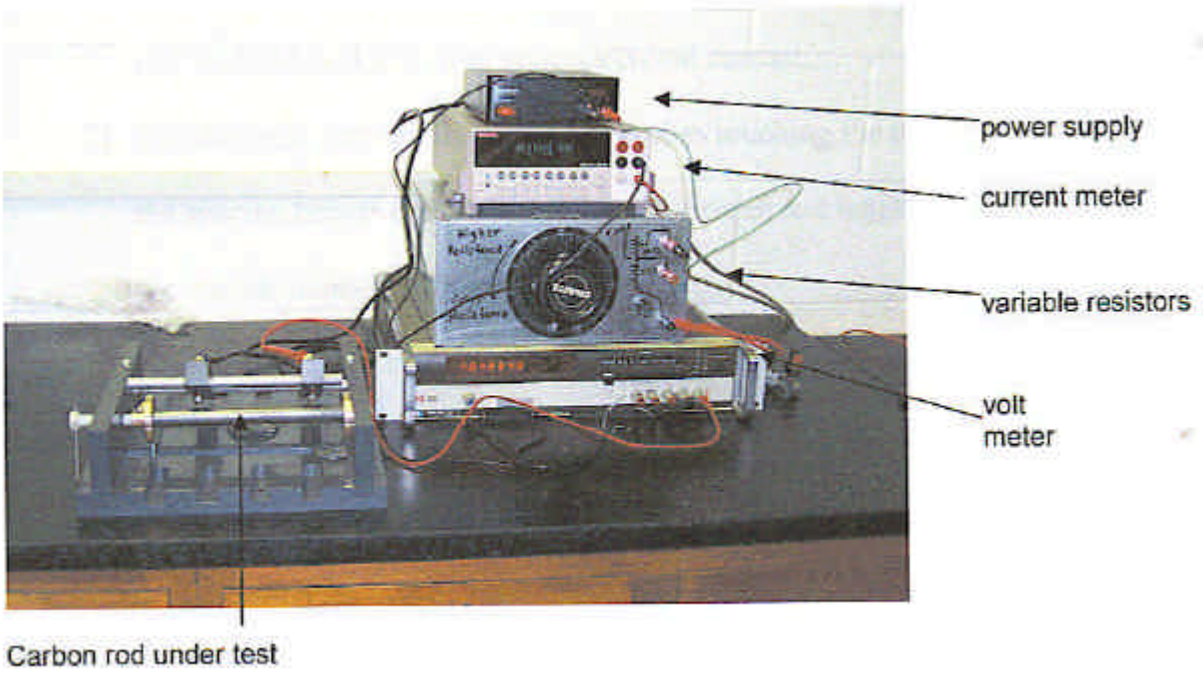

Figure 4. Rod Resistivity-Testing Apparatus.[1]

The current was measured by a digital amp meter (Keithley Model 2000) that is in series with the carbon fuel rod. The voltage drop across the rod was measured with a second digital volt meter (Keithley Model 2000) that is connected to the rod via two pointed contact pins over a measured distance. The circuit schematic is shown in Figure 5. The variable resistor allows for precise control of the current in the circuit.

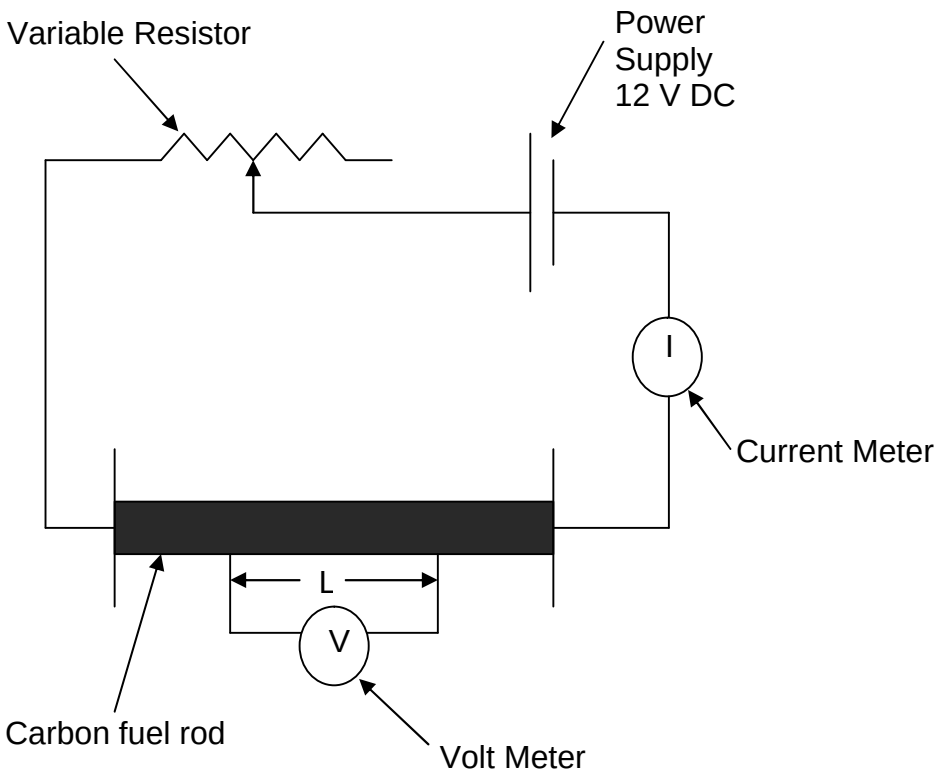

Figure 5. Schematic of Rod Resistivity-Testing Apparatus [1]

The proximate analysis is a set of procedures that determine moisture, volatile matter, ash content, and fixed carbon percentages in various coal and carbon materials. In the present research, a TGA 701 Thermo-Gravimetric analyzer by LECO is used according to the ASTM D 3174 method for ash determination. This instrument, shown in Figure 3.9, measures the weight loss of the sample as a function of temperature and time in a set atmosphere. About 2 grams of sample are placed in a silica crucible located on a rotating wheel which passes a balance as it rotates at a set frequency. Temperature profiles are monitored and recorded with the aid of an attached computer.

Figure 6. Leco TGA 701 Thermo-Gravimetric analyzer

2.1.2 Composite Elemental Analysis

Elemental analysis, also referred to as ultimate analysis, is used to determine the elemental composition of the sample with respect to carbon, hydrogen, sulfur, and nitrogen. Elemental analysis is carried out using a Thermoquest Inc. Flash EA-1112 CHNS-O elemental analyzer, shown in Figure 7. This instrument utilizes chromatography to determine the elemental content of a sample. The instrument is calibrated using a standard compound with known elemental composition. The sample is weighed in a tin container and dropped into the reactor, which is maintained at 900 ºC, where the sample combusts in the presence of excess oxygen in excess. The oxides that are produced are separated by the gas chromatograph and their relative amounts are determined by a thermal conductivity detector with reference to the standard.

Figure 7. Thermoquest Inc. Flash EA-1112 CHNS-O Elemental Analyzer

Rods were made with varying binder pitch levels to determine the lowest amount that would consistently yield a successful carbon fuel rod. Weight percent ranges from 5 to 25% were tested. The lowest amount of pitch blended with the other fuel ingredients that yielded a successful rod was found to be 10%. However, it proved difficult to work with that percentage as successful rods could not be consistently created. Thus, 15% binder pitch, by weight, was used for all subsequent rods.

Table 1 shows the elemental analysis and ash content for these Cenfuel/petcoke rods.

Table 1. Elemental Analysis and Ash Content for Cenfuel/Petcoke Rods (all rods contain 15% binder pitch by weight).

Coke Blend	N%	C%	H%	S%	Ash
0% Cenfuel,100% Petcoke	1.22	97.53	0.01	2.01	0.67
25% Cenfuel, 75% Petcoke	1.57	93.61	0.05	1.67	0.80
50% Cenfuel, 50% Petcoke	1.68	97.21	0.08	1.33	1.06
75% Cenfuel, 25% Petcoke	1.37	88.61	0.14	0.94	1.12
80% Cenfuel, 20% Petcoke	1.36	93.08	0.12	0.96	1.46
100% Cenfuel, 0% Petcoke	1.23	92.19	0.21	0.37	1.59

It is evident from this table that as the amount of Cenfuel increases in the rod, the ash increases and the sulfur content dramatically decreases, as is to be expected from the contents of the individual fuel ingredients.

Table 2 shows the elemental and proximate analysis for these SECO/petcoke rods. As with the Cenfuel/petcoke rods, with increasing SECO content in the rods, the sulfur decreases. However, the overall sulfur content is lower with the SECO rods than it is with the Cenfuel counterpart. The overall ash content for these rods is also lower than that observed with ones containing Cenfuel. This is due to the low ash and sulfur contents of both materials.

Table 2. Elemental Analysis and Ash Content for SECO/Petcoke Rods (all rods contain 15% binder pitch by weight).

Coke Blend	N%	C%	H%	S%	Ash
0% SECO, 100% Petcoke	1.22	97.53	0.01	2.01	0.67
25% SECO, 75% Petcoke	1.10	83.7	0.00	0.77	0.62
50% SECO, 50% Petcoke	1.26	87.6	0.00	0.45	0.54
75% SECO, 25% Petcoke	1.22	88.3	0.00	0.24	0.62
100% SECO, 0% Petcoke	1.46	90.8	0.01	0.23	0.54

2.1.3 Density and Resistivity

The density and the resistivity of the Cenfuel/petcoke rods were tested according to the methods described earlier. Table 3 shows the densities and resisitivities of the Cenfuel/petcoke rods.

Table 3. Resistivities and Densities of Cenfuel/Petcoke Rods

Rod	Resistivity (µ? -m)	Density (g/cc)
0% Cenfuel,100% Petcoke	202	1.52
25% Cenfuel, 75% Petcoke	317	1.41
50% Cenfuel, 50% Petcoke	298	1.23
75% Cenfuel, 25% Petcoke	235	1.25
80% Cenfuel, 20% Petcoke	140	1.40
100% Cenfuel, 0% Petcoke	109	1.36

It is not clear that there is a direct correlation between the Cenfuel content in a rod and its resistivity. However, the data suggests a decreasing resistivity with an increase in Cenfuel content.[1]

A plot of the resistivity of the rods against their densities also shows no evident correlation between these values, as can be seen in Figure 8. This is perhaps due to the small range of density variation within this group of rods. It is also feasible that the low resistivity of the Cenfuel/petcoke rods, regardless of content ratio, is due to the low resistivity of the binder pitch which is present throughout all the rods. Table 4 shows the densities and resisitivities of the SECO/petcoke rods.

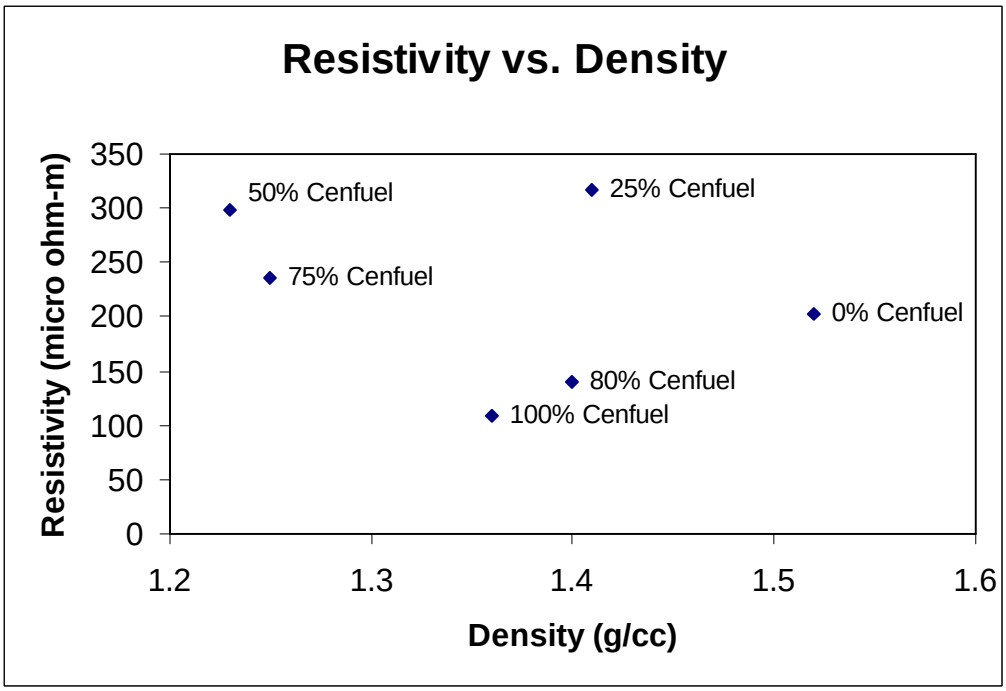

Figure 8. Cenfuel/Petcoke Rods: Resistivity vs. Density

Table 4. Resistvities and Densities of SECO/Petcoke Rods

Rod	Resistivity (µ? -m)	Density (g/cc)
0% SECO, 100% Petcoke	202	1.52
25% SECO, 75% Petcoke	136	1.53
50% SECO, 50% Petcoke	140	1.52
75% SECO, 25% Petcoke	78.6	1.43
100% SECO, 0% Petcoke	81.2	1.31

It appears that the resistivity of the rods goes down as the SECO content increases. The overall resistivity for the SECO rods is less than that of the petcoke ones. It is therefore a good candidate for low ash/low sulfur fuel.

Experiments with the fuel cell show that coal-derived material results in a significantly enhanced output voltage than obtained using graphite rods, as shown in Figure 9.

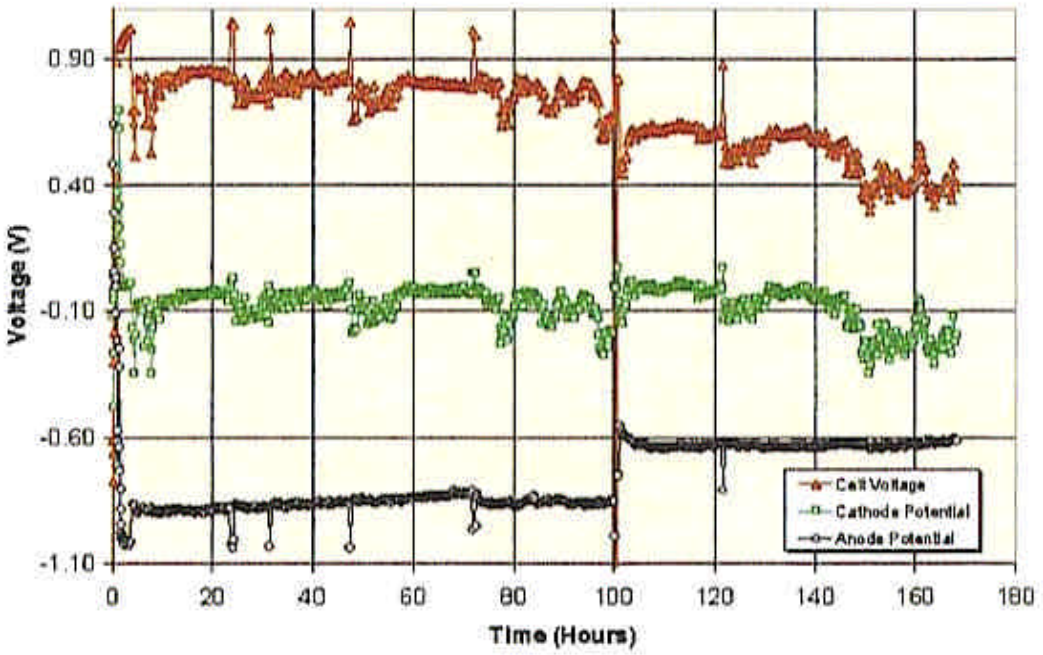

Figure 9. DCFC Performance with Coal-Derived Fuel vs. Graphite

The first 100 hours of Figure 9 portrays cell performance using a coal and petroleum coke derived anode, and for the remaining 70 hours, the same data are shown for a graphite anode. The overall cell voltage drops when the switch from the coal and petcoke to the graphite anode is made. Therefore it is clear that in this DCFC, coal performs more favorably than graphite.

Figure 10 shows the polarization curves (half-cell voltage with respect to a reference electrode vs. current) for the Cenfuel/petcoke rods at 600 ºC in NaOH+LiOH melt at a humidified airflow of 0.5 liters per minute at 70 ºC.

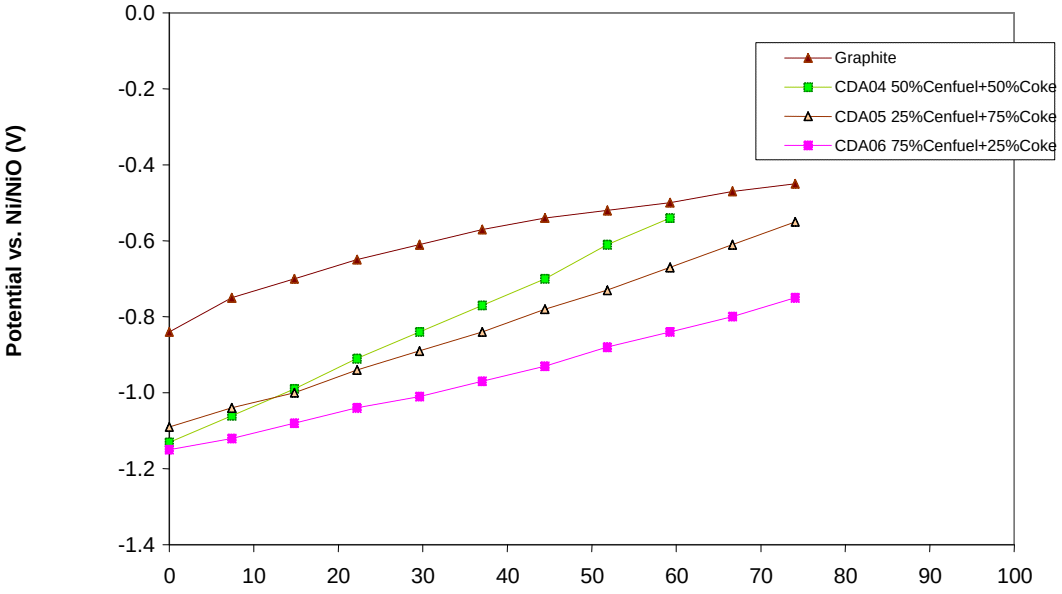

Figure 10. Anode Polarization Curves for Cenfuel/petcoke Fuel Rods at 600 ºC in NaOH+LiOH melt, 0.5l/min airflow humidified at 70ºC

As can be seen from the anode potential, the higher the Cenfuel content is correlated to a more negative half cell voltage. Although the graphite anode has a lower resistivity, its electrochemical activity in the cell pales to that of the Cenfuel anodes. The anode potentials of all the Cenfuel rods in Figure 10 are quite different; this supports the notion that the petcoke used in the rods is not the main cause of lowered resistivity. It is more likely that the binder pitch and/ or the Cenfuel are the major resistance-lowering factors. The behavior differentiating between the Cenfuel/petcoke rods can be attributed to Cenfuel's high electrochemical reactivity.

The apparent resistivity of the petcoke used in this research was higher than expected for anode coke. Hence it is possible that the petcoke was actually fuel grade rather than anode grade. The SECO not only had low sulfur content but outperformed both the 100% Cenfuel and 100% petcoke rods in terms of lower ash content and lower electrical resistivity. Preliminary fuel cell tests indicate that the rods containing coal-derived material have excellent electrochemical activity in their DCFC. This suggests that that SECO could be a candidate fuel for the DCFC, especially in situations requiring higher performance.

2.2 Carbon Foam Composites

Carbon foam was tested for ballistic characteristics.[2] With the United State's involvement in Middle Eastern conflict, the demand for personnel armor has increased. This may demand could possibly be met by the use of carbon foam composites. Another important aspect of this research is to determine possible applications for carbon foam.

While carbon foam is not expected to be an outright Kevlar replacement, it is believed that this research will prove that carbon foam exhibits impressive crushing and energy dissipation characteristics.[2]

In order to test the effectiveness of carbon foam in ballistic protection, samples that implement the carbon foam must be compared with samples that do not contain carbon foam. Thus, two types of samples were made. One type was made of a composite of aluminum plating, Kevlar, carbon foam, and Velcro cloth backing. The other type was the same as the first except the carbon foam was replaced by Kevlar of an equivalent weight. Therefore, all test samples had the same frontal area and the same mass.

The armor samples were made up of an aluminum front plate, layers of Kevlar, carbon foam, and a backing layer of Velcro cloth. The aluminum front plate was made of 5086 aluminum, which is as a ballistic grade metal. For example, it is used M-113 A3 armored vehicle. The front plates measured 9 inches by 9 inches and were approximately 5 mm thick. The Kevlar selected is also ballistic grade. It was purchased in 12 yard rolls and cut to 9.25 inch by 9.25 inch sections. Two types of carbon foam were used. The layer behind the aluminum front plate was of a higher density. The higher density foam was of higher strength than the lower density foam. Therefore it was used behind the aluminum where mushrooming of the bullet was important. All carbon foam layers are 5 mm thick. The Velcro cloth was cut to the same dimension as the Kevlar. The Velcro cloth was selected as a backing material to allow the armor sample to be mounted against either personnel protection or a vehicle. It was not expected to supply any ballistic protection.

The various layers of the armor pieces were held together by gluing the perimeter of the adjacent layers together with a piece of plastic wrap between each layer. A strong multipurpose adhesive called Gorilla Glue was used. The plastic wrap was used to decrease the amount of friction between the layers, thus allow each layer to react to the bullet individually.

The blunt trauma was measured using clay to absorb shock behind the armor sample, which was laid flush against it. The indentation of the clay is used as a measure of the shock that would be transmitted to a person or thing being protected. The non-drying clay is molded to a flat face inside plastic boxes. A sample of the clay backing box and an armor sample is shown in Figure 11.

Figure 11. Sample of ballistic armor and clay backing box

2.2.1 Manufacturing Protocol for Armor Containing Carbon Foam

The first step was to manufacture the armor samples according to the layer specifications shown in Figure 12.

Aluminum (9" x 9")
Foam (35lb/ft^3)
Kevlar, 8 layers
Foam (15lb/ft^3)
Kevlar, 4 layers
Foam (15lb/ft^3)
Velcro

Figure 12. Armor layer composition schematic

For the carbon foam armor samples, the 8 layer and 4 layer sections of Kevlar were first created. These sections were created by taking a single layer of Kevlar and applying the adhesive to the perimeter of the Kevlar. A piece of plastic wrap was placed between each piece of Kevlar and the next piece of Kevlar was then applied to the section. Finally, there were the 7 sections outlined in Figure 12 and shown in Figure 13.

Figure 13. The armor samples (containing carbon foam) shown in sections

The final constructed carbon foam armor samples are shown in Figure 14, Figure 15, and Figure 16. This is the back view of the samples. This is the face that is against the clay backing.

Figure 14. Carbon foam armor sample #1 (back view).

Figure 15. Carbon foam armor sample #2 (back view).

Figure 16. Carbon foam armor sample #3 (back view).

The three ballistic samples containing carbon foam were then weighed to determine how many layers of Kevlar needed to be included into the control sample that is made up of only aluminum, Kevlar, and Velcro. The weights of the carbon foam ballistic armor samples are shown in Table 5.

Table 5. Weights of carbon foam ballistic samples

Sample	Weight (g)
Sample #1	1554
Sample #2	1560
Sample #3	1612

By knowing these weights, and the weights of the aluminum plate and Velcro cloth to be used on the control sample, the number of layers of Kevlar needed to give a comparable

comparison could be determined. It was determined that 21 layers of Kevlar would give a weight very close to the 1575 gram average weight of the carbon foam samples.

The control sample that contains only the aluminum plating, 21 layers of Kevlar, and Velcro cloth backing is shown in Figure 17.

Figure 17. Armor control sample (back view).

The testing was to be done in a shooting range owned and operated by David Marstiller. He graciously lent his services and facility to test the samples. The clay backing box and samples were secured approximately 15 yards down the firing range from the firing booth. The test samples were held vertically, with the aluminum front plate facing toward the booth. The orientation of the sample and the clay backing box is shown in Figure 18.

Figure 18. Orientation of armor sample and clay backing box

2.2.2 Testing of Carbon Foam Samples

The next step was to test all four ballistic samples. There were two different types of tests completed: Preliminary Testing and Final Testing. The preliminary pistol and rifle testing was done to determine where the current armor configuration would best be tested in accordance to the NIJ Standard 0101.03.[3] The rifle testing was to determine how the armor sample would react against the AR-15 military rifle round. Designing a piece of body armor to stop a military rifle round was part of the motivation for the entire test sequence. The final testing compared the samples containing carbon foam to the samples that did not contain a carbon foam component.

The preliminary testing was accomplished with pistol rounds within the NIJ Type IIIA range and a rifle round within the NIJ Type III range. A high velocity 9mm round and a high velocity 357 Magnum round were fired into Carbon Foam Sample #3. The high velocity 9mm round is rated at approximately 1300 ft/s (396 m/s). This is a 125 grain (8.099 g) round. This is above Type II classification, but within Type IIIA classification. The 357 Magnum round is rated at 1450 ft/s (441 m/s) and has a nominal mass of 125 grains (8.099 g). This is above the Type IIIA requirements. The .223 military rifle round was from an AR-15. This was fired into Carbon Foam Sample #1. (NIJ 0101.04, 2001, p. 14)

The firing sequence for the preliminary testing is shown in Table 6.

Table 6. Firing Sequence for Preliminary Testing

Shot Number	Sample	Round
1	Carbon Foam Sample #3	9mm HV
2	Carbon Foam Sample #3	357 Mag
3	Carbon Foam Sample #1	AR-15

The reaction of the samples to the rounds determined what round would be used in the final testing. The highest rated round that left an obvious impact crater on the clay backing was chosen for the final testing.

The results of the preliminary testing determined that a high velocity 357 Magnum would be the best round to use for comparing carbon foam a ballistic armor sample to the control sample. The 357 Magnum round had a nominal mass of 125 grains (8.099 g) and a velocity of 1450 ft/s (441m/s). There were a total of 8 rounds fired into the various samples used: Carbon Foam Sample #1, Carbon Foam Sample #2, and the Control Sample.

The overall firing sequence for the final testing is shown in Table 7. Please note that all 357 Magnum rounds were of the same velocity and nominal mass.

Table 7. Firing Sequence for Final Testing

Shot Number	Sample	Round
1	Carbon Foam Sample #1	357 Magnum
2	Carbon Foam Sample #1	357 Magnum
3	Control Sample	357 Magnum
4	Control Sample	357 Magnum
5	Control Sample	357 Magnum
6	Carbon Foam Sample #2	357 Magnum
7	Carbon Foam Sample #2	357 Magnum
8	Carbon Foam Sample #2	357 Magnum

The depth of the impact craters created by the blunt trauma was measured as an indicator of damage. The results of the preliminary testing were analyzed based on the extent of damage to the armor. Obviously, nothing can be learned if the armor is completely destroyed, or completely undamaged. Thus, to compare the effectiveness of the samples, the round closest to causing complete failure in the carbon foam sample was used to test the remaining carbon foam samples and the control sample.

The results of the final testing were analyzed based on the depth of the resultant blunt trauma crater in the clay. The actual depths will be compared to determine how close the carbon foam ballistic samples are in terms of performance to the control sample.

The first round fired was the 9mm (high velocity). It did not penetrate the aluminum, as shown in Figure 19. The aluminum layer was removed to see the reaction of the foam to the impacts, which is shown in Figure 20. A close up of the reaction to the 9mm round is shown in Figure 21. The clay backing had no indentation from the 9mm round.

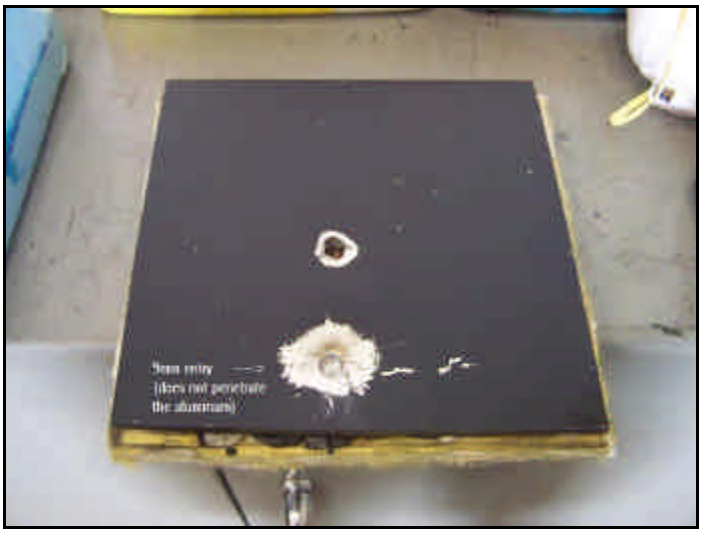

Figure 19. Point of entry for the 9mm round into Carbon Foam Sample #3

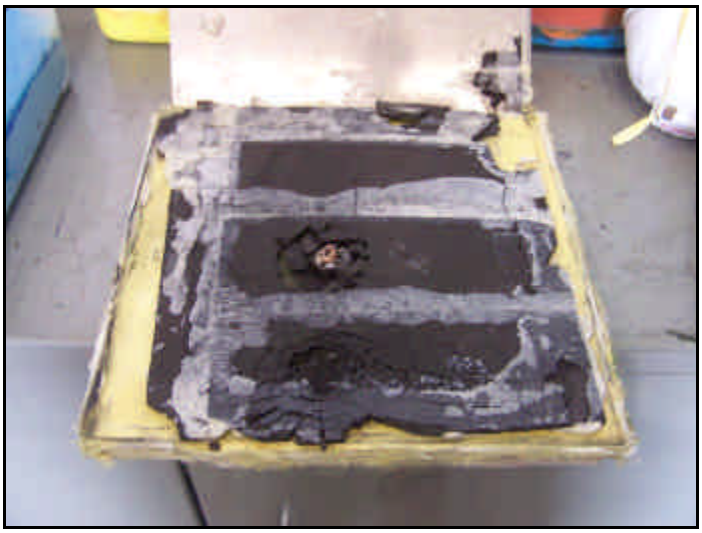

Figure 20. Reaction of carbon foam to the 9mm round (bottom) and the 357 Magnum round (top) in Carbon Foam Sample #3.

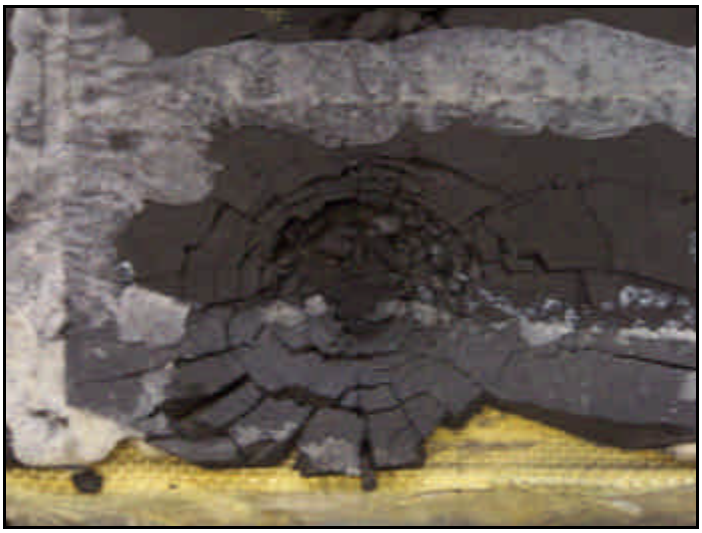

Figure 21. Damaged carbon foam layer from a 9mm round in Carbon Foam Sample #3.

The second shot fired was the 357 Magnum. The initial point of entry into the metal is shown in Figure 22. It was a clean cut through the metal. Upon examination of the actual bullet, it could be seen that the bullet sheared completely through the aluminum faceplate. The sheared aluminum was packed on the front portion of the bullet. The reaction of the first layer of foam and Kevlar from the 357 Magnum round is shown in Figure 23.

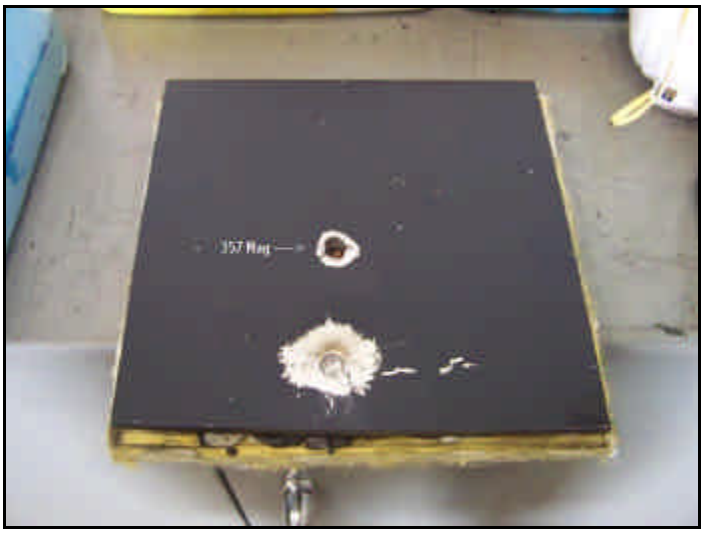

Figure 22. Point of entry for the 357 Magnum round on Carbon Foam Sample #3

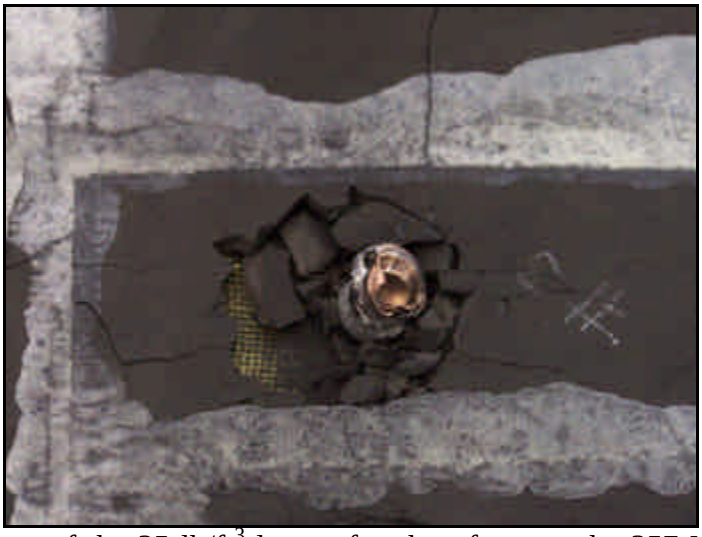

Figure 23. Damage of the 35 lb/ft^3 layer of carbon foam to the 357 Magnum round in Carbon Foam Sample #3.

Once the crushed foam was removed, the first layer of Kevlar showed some tensile damage to the fiber matrix, as seen in Figure 24.

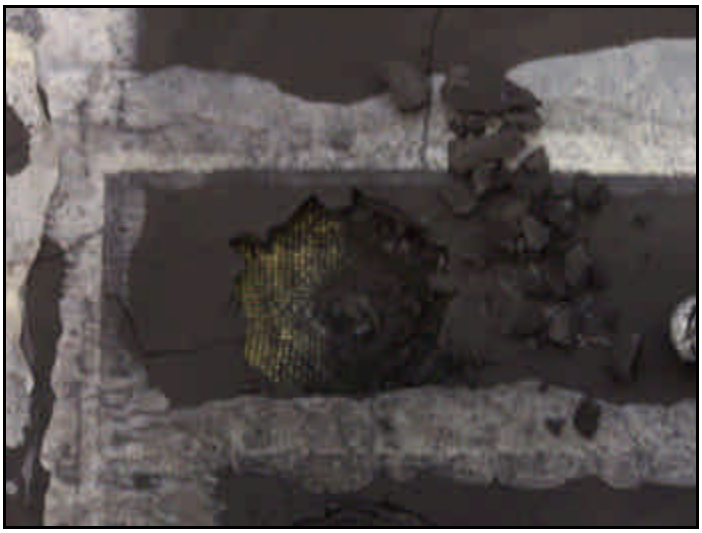

Figure 24. Damage to 8 layer section of Kevlar from the 357 Magnum round.

The clay backing showed an indentation from the 357 Magnum round. The depth of penetration was 0.3985 inches. The Velcro backing of the armor sample permitted us to see how the back layer of foam reacted. Directly behind where the bullets hit the front plate, crushed foam can be felt. Even though the bullet never reached the back or middle layers, we could feel a similar crush style to the back layer of carbon foam.

For the rifle round (AR-15, .223), carbon foam sample #1 was completely pierced by the bullet as shown in Figure 25 and Figure 26. The bullet continued out the back of the armor completely through the clay backing as well. This is shown in Figure 27.

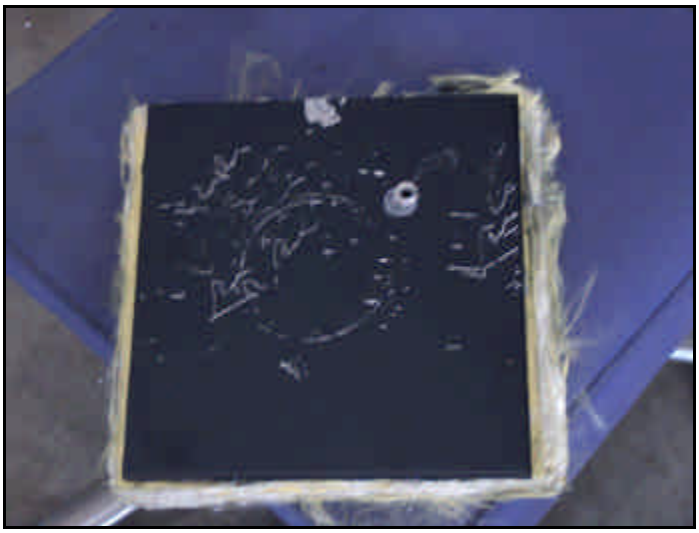

Figure 25. Point of entry to AR-15 (.223) round into Carbon Foam Sample #1.

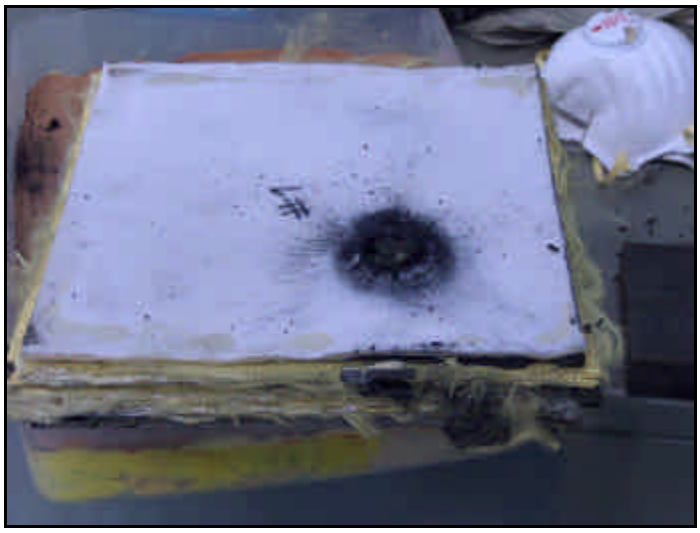

Figure 26. Exit hole created by the AR-15 (.223) on Carbon Foam Sample #1.

Figure 27. Penetration of the AR-15 round through the clay backing for Carbon Foam Sample #1.

These preliminary testing results were used to determine what round to do the final testing with.

The 8 shots fired into the carbon foam sample #1, carbon foam sample #2, and the control sample were all considered survivable shots. The actual depth into the clay, from blunt trauma, is shown in Table 8 These are all well below the allowable 1.7 inch depth permitted by National Institute of Justice (NIJ) testing standards.

Table 8. Depth of penetration into the clay backing from blunt trauma

Shot Number	Sample	Round	Location on Face of Sample	Depth (in)
1	1	357 Mag	center-middle	0.455
2	1	357 Mag	left-middle	0.521
3	control	357 Mag	right-middle	Less than 0.100
4	control	357 Mag	center-middle	Less than 0.100
5	control	357 Mag	left-top	Less than 0.100
6	2	357 Mag	left-top	0.360
7	2	357 Mag	center-middle	0.355
8	2	357 Mag	right-bottom	0.553

The damage to the whole assembly of carbon foam sample #1 can be seen in Figure 28. The damage to the foam directly behind the aluminum plating is shown in Figure 29 as the damage to the second layer of carbon foam is shown in Figure 31. The impact effect on the Kevlar layer (8 layers) is shown in Figure 30. Figure 32 shows the blunt trauma affect on the clay backing.

Figure 28. Carbon Foam Sample #1 after being tested with 357 Magnum rounds and AR-15 round.

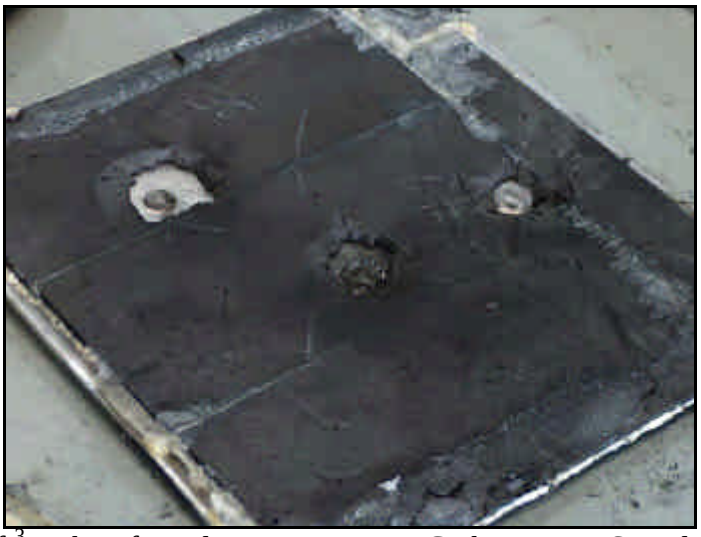

Figure 29. 35 lb/ft^3 carbon foam layer reaction on Carbon Foam Sample #1 (viewed from behind).

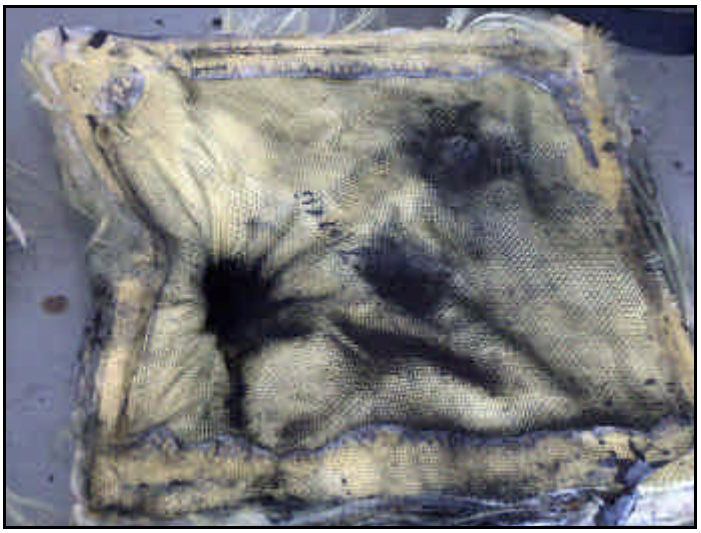

Figure 30. Reaction of the 8 layer Kevlar section on Carbon Foam Sample #1.

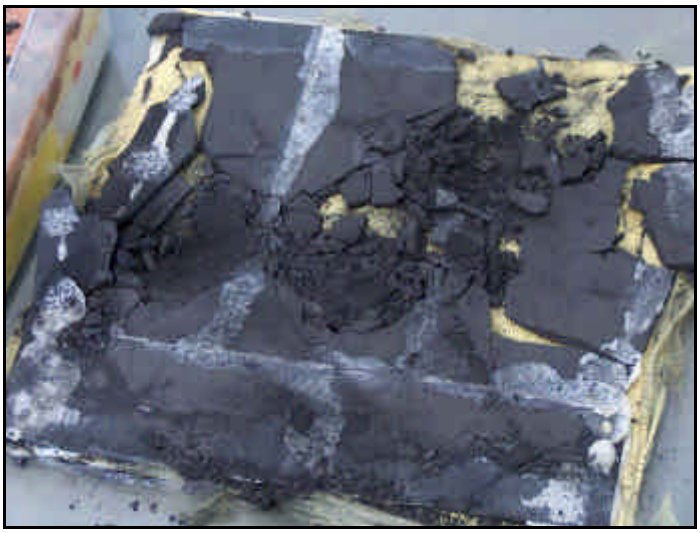

Figure 31. Reaction of the middle layer of carbon foam on Carbon Foam Sample #1.

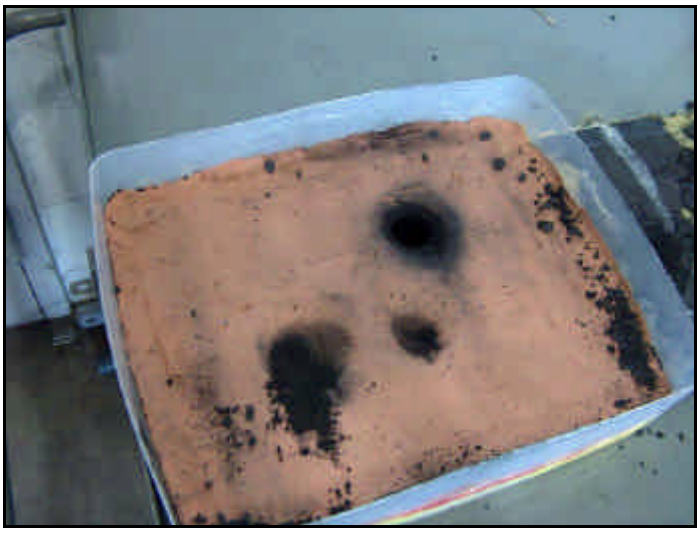

Figure 32. Blunt trauma reaction to 357 Magnum rounds on Carbon Foam Sample #1.

The control sample reaction is shown in Figure 33 and the imprint into the Kevlar is shown in Figure 34. The shells did not penetrate the aluminum plating, as compared to carbon foam sample #1 and carbon foam sample #2. The depth of the crater in the clay was not measurable.

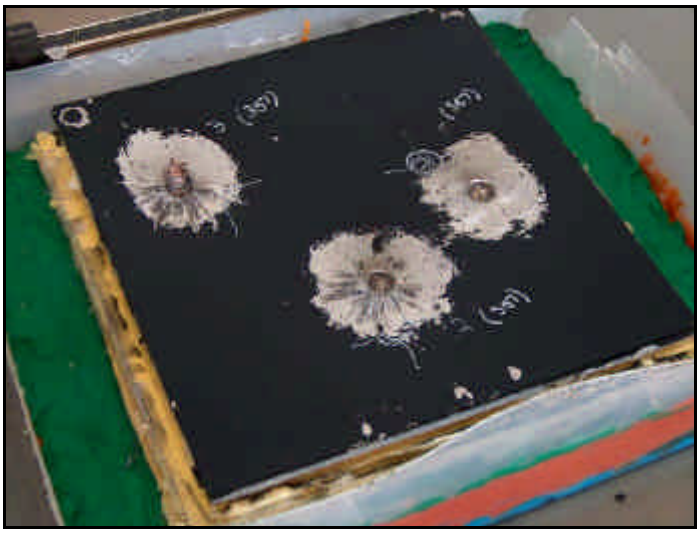

Figure 33. Points of contact on the Control Sample by the 357 Magnum rounds.

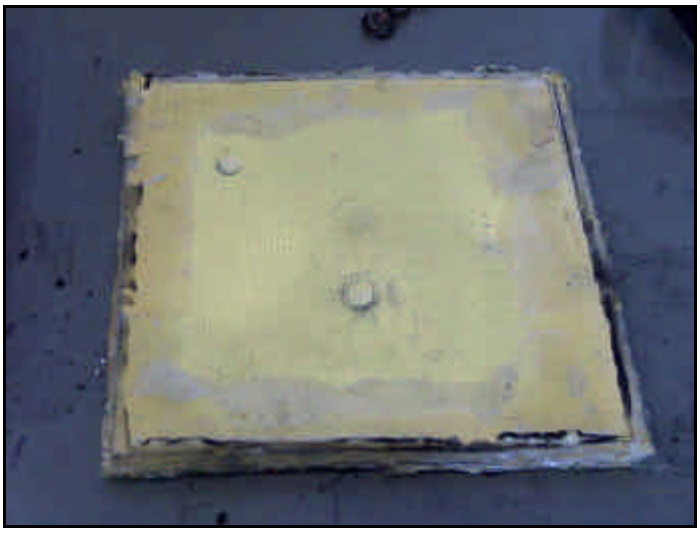

Figure 34. Kevlar's reaction to the 357 Magnum rounds on the Control Sample.

The reaction of carbon foam sample #2 is shown in Figure 35 through Figure 38. Figure 35 shows the points of entry on carbon foam sample #2. The reaction of the 35 lb/ft^3 layer is shown in Figure 36. The 8 layers of Kevlar section is seen in Figure 37. The bullet was stopped by the 8 layers of Kevlar but crushing effect was shown in both 15 lb/ft^3 carbon foam layers. The reaction of the middle layer of carbon foam is illustrated in Figure 38. Finally, the blunt trauma indentions can be seen in Figure 39.

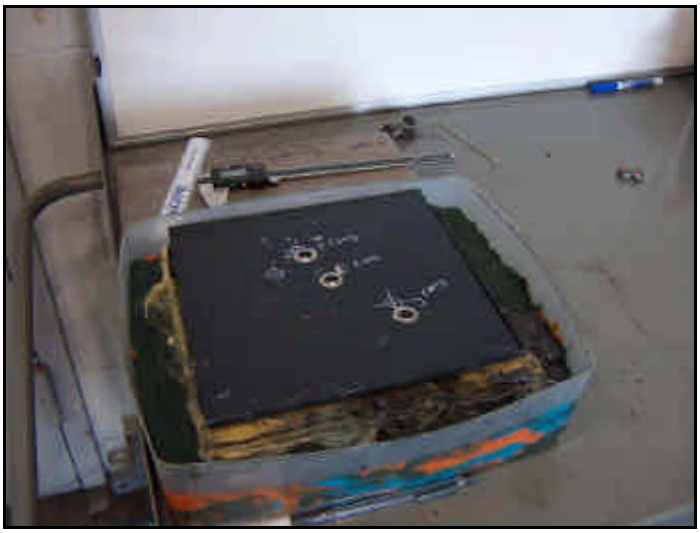

Figure 35. The complete assembly of Carbon Foam Sample #2.

Figure 36. The back view of Carbon Foam Sample #1's first layer of carbon foam.

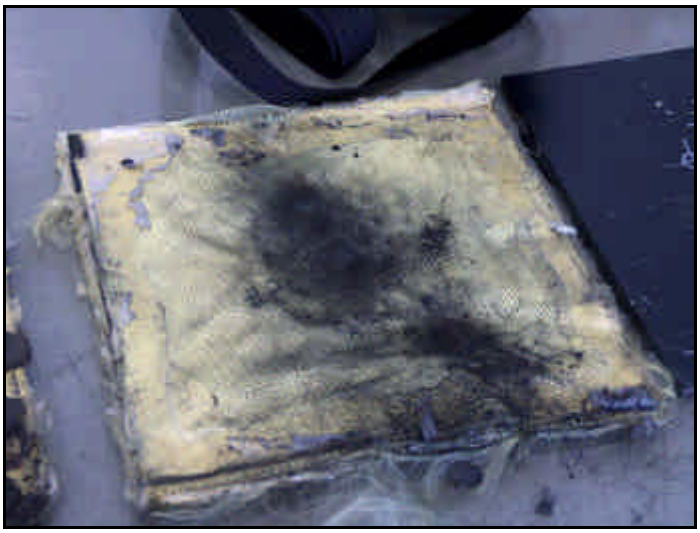

Figure 37. The 8 Kevlar layer's reaction of Carbon Foam Sample #2.

Figure 38. The second layer of carbon foam reaction on Carbon Foam Sample #2

Figure 39. The clay backing blunt trauma reaction for Carbon Foam Sample #2

2.2.3 Observations on Carbon Foam Armor

The tests give very concrete indications that Kevlar was generally more effective than carbon foam under the conditions tested. The depth of the blunt trauma craters was smaller in the control sample than the samples containing carbon foam. This alone indicates that for the particular use of personal ballistic protection, multiple layers of Kevlar is the superior ballistic resistant panel. The fact that the Kevlar samples were physically thinner than the carbon foam samples is another positive for Kevlar, especially for personnel armor applications. Less bulky armor allows for better movement for those who wear the armor.

These findings do not discount carbon foam as a form of energy dissipation via crushing though. When comparing the faceplates of the carbon foam samples, as in Figure 28 and Figure 35, to the faceplate of the sample containing only Kevlar, as in Figure 33, it is visible that the area around in point of entry on the carbon foam samples has a smaller ring of paint removed. The sample that contains only Kevlar shows a larger diameter ring of paint removed around the point of entry. The paint removal is an indication of deflection of that area of the faceplate. It is believed that the carbon foam directly behind the aluminum retarded the ductile properties of the aluminum. In a situation with such a severe impact as ballistics, this phenomenon could have had a negative impact on the carbon foam samples' ability to be effective in ballistic protection. It is recommended that future research of carbon foam in ballistic armor should have a layer between the carbon foam and the metal faceplate. The data from Xu and Rosakis's study of impact induced multilayer failure should also be reviewed for energy translation between layers.[4]

The abilities represented by the carbon foam as a crushing material are estimated to be of interest for other applications, however. Due to the fact that carbon foam has a low density, it could be used in the door panels of military vehicles. In these situations, minimal weight is more important than volume and comfort, as personal ballistic armor

is. Forming carbon foam into complex shapes is rather simple and could be done using basic machining processes with minimal wear on the machining components. Another possibility for carbon foam is within the walls of blast rooms. The fact that large pieces of carbon foam are easy to manufacture makes it a prime candidate for blast rooms.

2.3 Solvent Hydrotreating

Currently hydrotreating is carried out in Room 317, Engineering Research Laboratory. Several modifications were made to the system, as shown in Figure 40. Specifically,

a. A pressure relief valve (PRV) was added to the hydrotreating reactor, in series with the original equipment manufacturer's rupture disk. The rupture disk is designed to yield at 3000 psig. When a flammable mixture is used, however, a rupture disk is not necessarily the best solution, because it results in immediate dispersion of the flammable mixture throughout the fume hood; should that somehow ignite. Accordingly, the PRV permits only the excess gas to be released, and then continues to hold pressure. By more slowly venting the excess gas to the fume hood, it is possible to remain below the lower explosive limit (LEL) at all times. In addition, a pressure gauge is installed between the rupture disk and PRV. Thus, when the rupture disk yields, the pressure gauge reads some finite pressure, providing the operator a sign that the rupture disk has yielded.

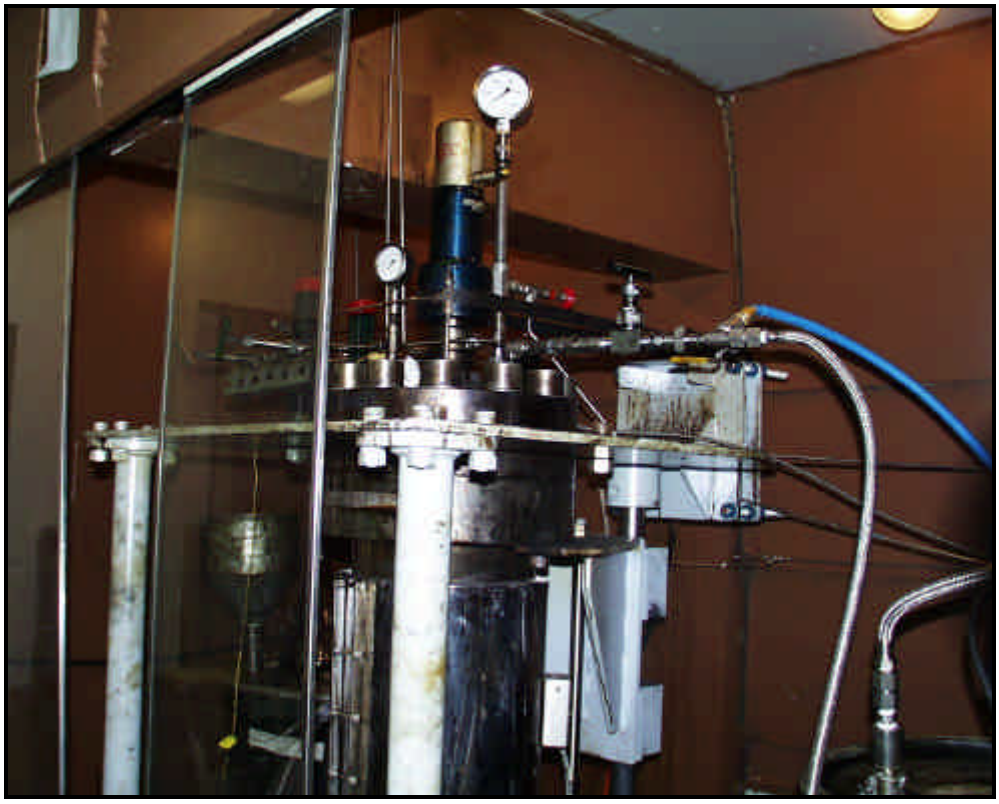

Figure 40. Hydro-Treatment Reactor, with Pressure Relief Valve and Gauge visible in the background.

c. A holding tank is used to allow the operator to vent gases from the reactor. The volume of the holding tank is 50 gallons and the pressure rating is 200 psig. At ambient temperature, this corresponds to 3200 standard liters. By comparison, during normal operation the reactor should have no more than about 1.5 gallons of head space at 2000 psig or less, corresponding to 232 standard liters. Even if the reactor were to be (accidentally) filled with pure hydrogen at 3000 psig, this is still only 350 standard liters. This way, in the unlikely event that the reactor were to suddenly release all of its contents, the contents would not be dispersed into the fume hood, but instead would be contained in the holding tank. It would then slowly vent through a needle valve and flame arrestor at the top of the tank.

Figure 41. The blue tank in the rear is a holding tank to allow vented gas to be temporarily stored and slowly vented.

d. The purpose of the flame arrestor is to ensure that, in the unlikely event that air is mixed with the hydrogen and coal tar vapors, and is somehow ignited, the flame will not propagate back through the piping to the holding tank or the reactor.

e. A grounding cable was added between the reactor and the product holding tank (that is, a 55 gallon drum that contains the product). This assures that a potential difference can not be created between the product and the holding tank, minimizing the probability of a static discharge.

f. A tank of water was added to cool the product as it is released from the reactor. The product leaves the reactor at 400 ^{o}C, and is now cooled to about 100 ^{o}C or below at the exit point. The vessel itself is close to ambient temperature. By reducing the

temperature of the product, the vapor pressure is reduced and the chances of reaching an explosive or flammable concentration of vapor is minimized.

g. An additional planned step will be to continuously bleed a small amount of nitrogen to the product tank, thus inerting the contents and reducing the ability of the atmosphere to feed any fire or explosive situation that might otherwise be created.

h. The power cable is now doubly insulated, using a PVC duct to protect it against "wear and tear." Thermal insulation is used to ensure that the product line can not accidentally contact the polymer insulation and melt it.

i. A pump has been installed between the neat solvent (Koppers coal tar distillate) and the reactor.

j. A drum scale is used to weigh the contents of the drum containing the neat solvent. Accordingly, it is possible to dispense a well-quantified amount of solvent. Currently the protocol is 26 lbs +/- 0.2 lbs, whereas previously it is estimated that only 17 lbs were processed.

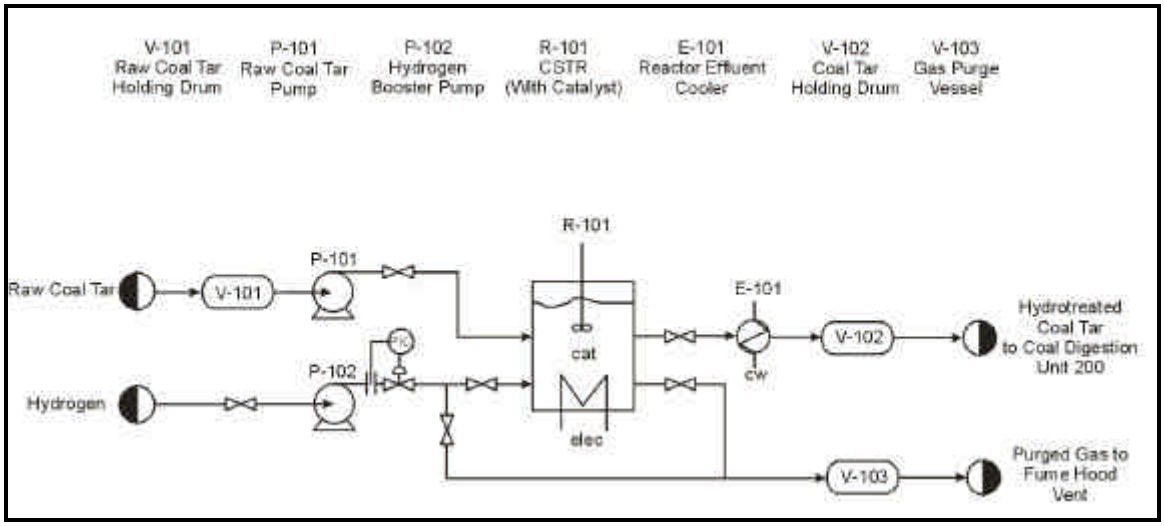

Figure 42. Modified Reactor System.

In the current configuration, it is possible to keep the reactor hot at all times, and to transfer coal tar distillate to the reactor without exposing the contents of the reactor to air. Consequently, semi-batch operation is possible. The time required to turn around the reactor from hydrogen shut-off to hydrogen turn-on is currently about 45 minutes. However, by using an intermediate holding tank to acquire the product, This time can probably be cut in half, limited mainly by the time required to heat up the contents of the reactor to the desired operating temperature (currently 400 to 415 ^{o}C).

Currently, the protocol is to pump 27 lbs of coal tar distillate in the reactor. The reactor is brought to temperature as quickly as possible. The sample is maintained at the desired operating temperature for a period of one to three hours, depending on the desired level of hydrogenation. Then a valve is opened to permit the product to be slowly released through a heat exchanger (heat-sunk to a water cooling bath) and then to the

product drum. Excess gas is vented to a holding tank. Then the reactor is refilled and the process is reinitiated.

The chief metric for success in hydrotreatment is the ratio of peaks in the Fourier Transform Infrared (FTIR) spectrum. Unfortunately, the Nicolet FTIR system used suffered an untimely demise and cold not be repaired due to its demise. Accordingly, the measurements have been switched to a Perkin-Elmer Spectrum One FTIR with manufacturer supplied (Spectrum) software. The measurements are presumed to be similar on the two machines, but a side-by-side comparison can not be made. Nuclear Magnetic Resonance (NMR) may yet be the preferred technique, but FTIR is preferred for daily operations because of the simplicity and speed of the measurements.

As shown in Figures 43 and 44, peak areas corresponding to aromatic and aliphatic molecules are compared. In each case the corrected area is used, in which the background spectrum is subtracted by linearly truncating the peak at the local minima. The ratio of aromatic to aliphatic hydrogen is an indicator of the extent to which hydrogen has been successfully absorbed in the solvent, which in turn is correlated to higher solubility of coal.

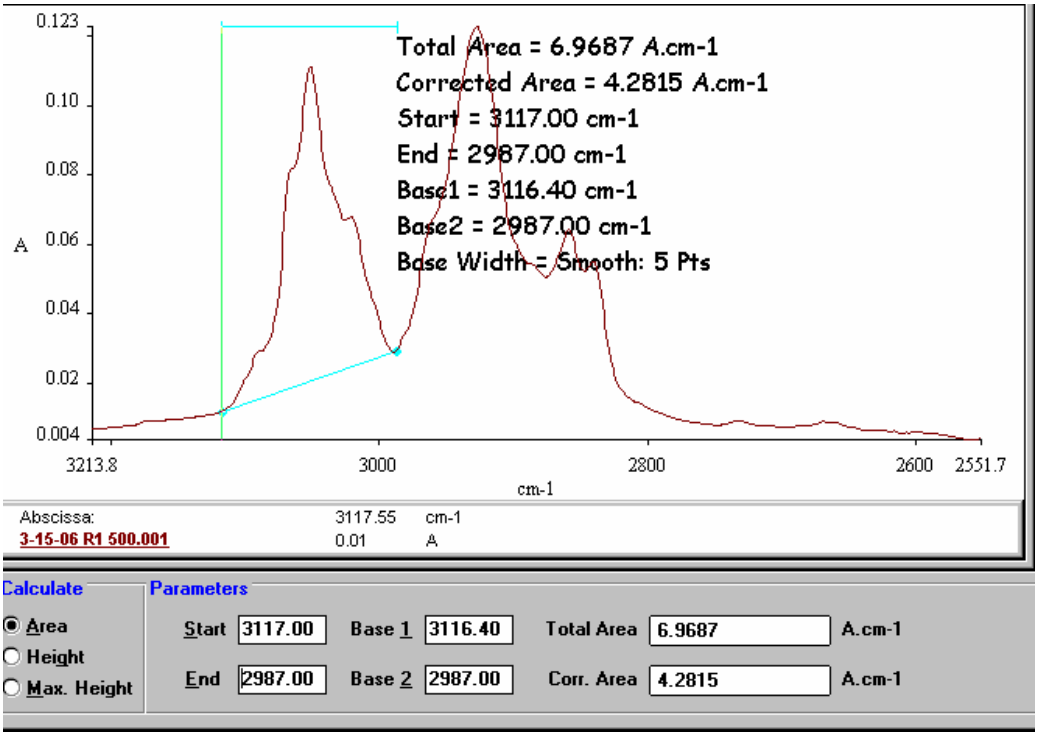

Figure 43. FTIR Peak Measurement of the peak area between 3117-2987 cm-1 (the "aromatic" fraction).

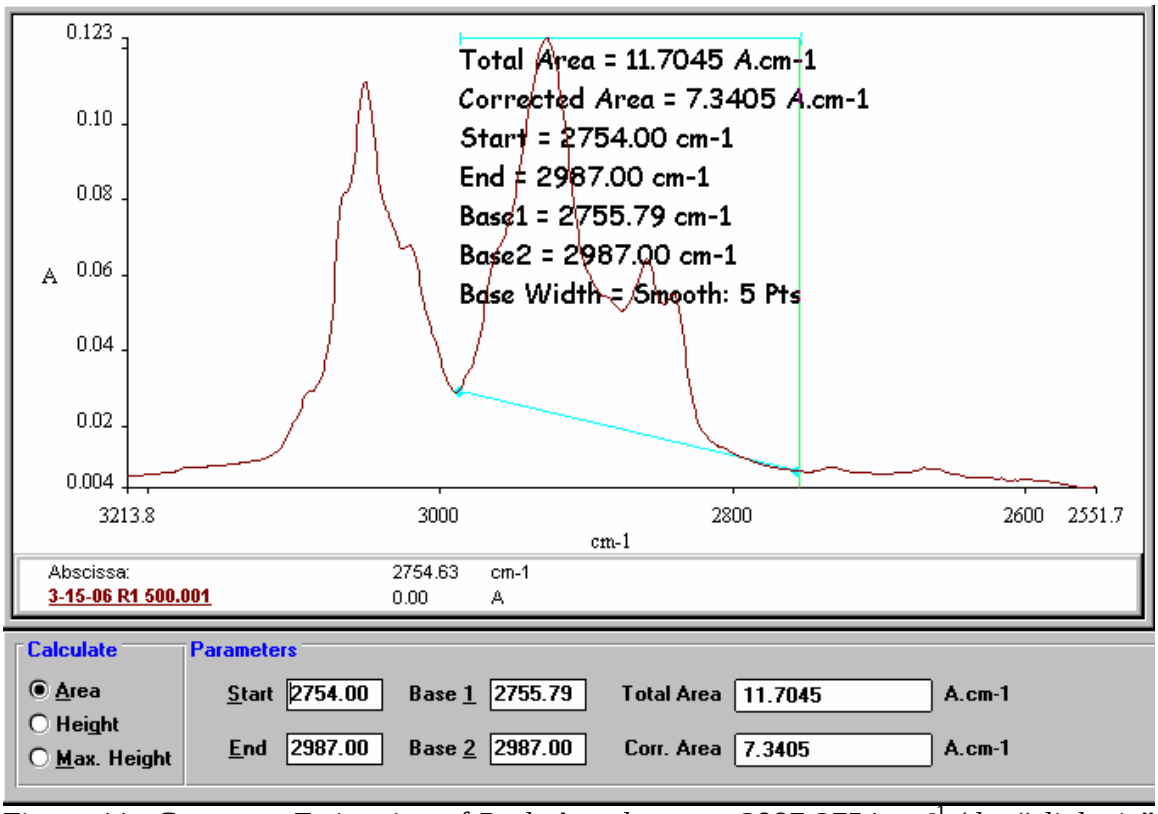

Figure 44. Computer Estimation of Peak Area between 2987-2754 cm^{-1} (the "aliphatic" fraction).

In semi-batch mode, the current protocol results in one hour operating time with 45 to 60 minutes time between operational runs. Consequently, it is possible to produce 4 x 27 lbs or 108 ponds per 8 hour shift assuming that no breakdowns occur. By shortening the time for removing the product, it is possible that about 6 runs per shift (144 lbs per shift) can be accomplished.

The project is currently scheduled to produce 1500 pounds of pitch, requiring approximately 3000 pounds of solvent. The baseline protocol will not be changed during this production run.

However, for future runs, he kinetics of the system can likely be affected by increasing the hydrotreatment temperature. If so, a shorter residence time is possible. This will If residence time can be decreased to 15 minutes, with load/unload times in the range of 5 minutes, as many as 20 runs possible in an eight hour shift, or 520 lbs.

True continuous operation can be accomplished by substituting a high pressure pump to supply coal tar distillate to the reactor, with a let-down pump at the reactor outlet to meter the output continuously.

3.0 Concluding Remarks

The main focus of this efforts continues to be the demonstration of binder pitch in commercial electrodes. This effort, if successful, will also allay most concerns pertaining

to related products such as binder pitch for commercial anodes for aluminum smelting, as well as impregnation pitch and other carbon products.

4.0 References

1. Saddawi, Abha, "Carbon Fuels for the Direct Carbon Fuel Cell", Thesis (MS), West Virginia University, 2005

2 . Berg, Quentin "Carbon Foam Composites in Ballistic Armor", Undergraduate Research West Virginia University, 2005.

3 . National Institute of Justice. 2001. *NIJ Standard-0101.04 Ballistic Resistance of Personal Body Armor.* Washington, DC: National Institute of Justice.

4. Xu, L. Roy and Rosakis, J. Ares. 2003. "An Experimental Study of Impact-induced Failure Events in Homogeneous Layered Materials using Dynamic Photoelasticity and High-speed Photography" *Optics and Lasers in Engineering* 40 (2003): 263-288.